

Gaussian Process-based Min-norm Stabilizing Controller for Control-Affine Systems with Uncertain Input Effects

Fernando Castañeda*, Jason J. Choi*, Bike Zhang, Claire J. Tomlin and Koushil Sreenath

Abstract—This paper presents a method to design a min-norm Control Lyapunov Function (CLF)-based stabilizing controller for a control-affine system with uncertain dynamics using Gaussian Process (GP) regression. We propose a novel compound kernel that captures the control-affine nature of the problem, which permits the estimation of both state and input-dependent model uncertainty in a single GP regression problem. Furthermore, we provide probabilistic guarantees of convergence by the use of GP Upper Confidence Bound analysis and the formulation of a CLF-based stability chance constraint which can be incorporated in a min-norm optimization problem. We show that this resulting optimization problem is convex, and we call it “Gaussian Process-based Control Lyapunov Function Second-Order Cone Program” (GP-CLF-SOCP). The data-collection process and the training of the GP regression model are carried out in an episodic learning fashion. We validate the proposed algorithm and controller in numerical simulations of an inverted pendulum and a kinematic bicycle model, resulting in stable trajectories which are very similar to the ones obtained if we actually knew the true plant dynamics.

I. INTRODUCTION

Model-based controllers have a problem inherent to their nature: model uncertainty. In this paper, we directly address this issue for the case of Lyapunov-based stabilizing controllers for nonlinear control-affine systems by using Gaussian Process (GP) regression to estimate the adverse effects of model uncertainty.

Control Lyapunov Functions (CLFs) [1], [2] have been widely used in recent years for nonlinear model-based stabilizing control of robotic systems [3], [4], [5]. Typically, the robot is stabilized by enforcing the CLF to decay to zero by designing a constraint in an optimization problem [6]. However, CLF-based optimization methods heavily rely on the assumption that the model used for the controller design accurately represents the true plant’s dynamics. If there is model-plant mismatch, convergence guarantees are often lost. Past research has directly addressed this issue by using both robust [4] and adaptive [7] control theory. More recently, various kinds of data-driven methods that use neural networks have been introduced [8], [9], [10]. Although these

are demonstrated to be effective in practice, they do not take into account the uncertainty of the learning outputs.

For this paper, we are more interested in another class of data-driven approaches to tackle this problem, which use Gaussian Process regression. GP regression allows for the analysis of the confidence of the learning prediction. The method of applying GPs to the CLF constraint was first introduced for closed-loop systems in [11]. Then, similar approaches have also been proposed for the construction of stability and safety constraints to be incorporated in min-norm controllers [12], [13], [14], [15]. However, all of these papers make an important assumption that might restrict their applicability, which is that the considered model uncertainty is unaffected by the control input. In contrast, for many controlled systems, uncertain input effects¹ are prevalent (e.g. in a mechanical system, uncertainty in the inertia matrix directly induces uncertain input effects). In the work presented in [16], a similar problem is addressed for the case of Control Barrier Function-based safety constraints [17] by the use of a matrix variate GP regression. However, this method does not provide a regression confidence analysis. Finally, all the aforementioned GP-based approaches apply GP regression directly to the dynamics vector fields, which scale poorly with the system dimension.

In this paper, we develop solutions to overcome the presented limitations of the previous GP-based methods. First, we provide a formal way to deal with input-dependent model uncertainty of control-affine systems by proposing a specific GP kernel structure suitable for this problem. Also, since we apply GP regression to the uncertainty term in the CLF constraint, which is a scalar value, our regression problem is of lower dimension than if we directly learned the uncertain portion of the dynamics of the system. Additionally, we formulate a Second-Order Cone Program (SOCP) optimization problem which incorporates a chance constraint that takes into account the regression error of the GP model and provides the exponential stabilizability of the system. We call it *Gaussian Process-based Control Lyapunov Function Second-Order Cone Program* (GP-CLF-SOCP). Formulation of the SOCP is crucial in that it can be solved quickly enough for real-time applications. Finally, since the inference time of GP regression is directly determined by the size of training data, we maximize data efficiency by the use of an algorithm that iteratively collects data and improves the GP regression model in an episodic learning fashion.

The rest of the paper is organized as follows. In Section

*Indicates equal contribution.

Fernando Castañeda, Jason J. Choi, Bike Zhang, Claire J. Tomlin and Koushil Sreenath are with the University of California, Berkeley, CA, 94720, USA. {fcastaneda, jason.choi, bikezhang, tomlin, koushils}@berkeley.edu

This work was partially supported through National Science Foundation Grant CMMI-1931853. The work of Fernando Castañeda received the support of a fellowship from Fundación Rafael del Pino, Spain. The work of Jason Choi received the support of a fellowship from Kwanjeong Educational Foundation, Korea.

¹Uncertainty in the control vector field $g(x)$ in (1).

II, we give a brief overview of CLF-based controllers and show the effects that model uncertainty has on them. In Section III, we explain the basic concepts of GP regression. In Section IV, we present the compound kernel structure that allows us to regress the control-affine uncertainty. In Section V, we present the SOCP formulation of our uncertainty-aware optimization problem. In Section VI, we propose an efficient data-collection procedure. In Section VII we validate the proposed method for two different systems. Finally, in Section VIII, we provide concluding remarks and future work directions.

II. PROBLEM STATEMENT

Throughout this paper we will consider nonlinear control-affine systems of the form

$$\dot{x} = f(x) + g(x)u, \quad (1)$$

where $x \in \mathbb{R}^n$ is the state of the system and $u \in \mathbb{R}^m$ is the control input. The vector fields $f: \mathbb{R}^n \rightarrow \mathbb{R}^n$ and $g: \mathbb{R}^n \rightarrow \mathbb{R}^{n \times m}$ are assumed to be locally Lipschitz continuous and $f(0) = 0$.

The main objective of this paper is the construction of a locally stabilizing controller for such a system even when its dynamics are uncertain. A system is called *stabilizable* when it is asymptotically controllable to the origin with a feedback control law $u: \mathbb{R}^n \rightarrow \mathbb{R}^m$ that is continuous except possibly at the origin.

A. Control Lyapunov Functions

Definition 1. Let $V: \mathbb{R}^n \rightarrow \mathbb{R}_+$ be a positive definite, continuously differentiable and radially unbounded function. We say that V is a *Control Lyapunov Function* (CLF) for system (1) if for each $x \in \mathbb{R}^n \setminus \{0\}$

$$\inf_{u \in \mathbb{R}^m} \underbrace{L_f V(x) + L_g V(x)u}_{=\dot{V}(x,u)} < 0, \quad (2)$$

where the functions $L_f V(x) := \nabla V(x) \cdot f(x)$ and $L_g V(x) := \nabla V(x) \cdot g(x)$ are known as Lie derivatives.

If such a CLF exists, the system is known to be globally stabilizable [1]. Then, it is desirable to find a locally Lipschitz continuous feedback control law $u: \mathbb{R}^n \rightarrow \mathbb{R}^m$ such that the condition $L_f V(x) + L_g V(x)u(x) < 0$ holds for any $x \in \mathbb{R}^n \setminus \{0\}$. A simple way of synthesizing such a control law is by enforcing (2) as a constraint in a min-norm optimization problem. If u is unconstrained, this min-norm stabilizing controller can be expressed in closed-form [2].

However, many real-world systems require the addition of input constraints due to actuator limitations, i.e., $u \in U \subset \mathbb{R}^m$, in which case condition (2) becomes $\inf_{u \in U} L_f V(x) + L_g V(x)u < 0$, which might not be satisfied at every $x \in \mathbb{R}^n \setminus \{0\}$ even if V is a valid CLF for system (1). This fact motivates the following lemma.

Lemma 1. Let $V: \mathbb{R}^n \rightarrow \mathbb{R}_+$ be a CLF for system (1) and let $U \subset \mathbb{R}^m$ be the compact set of admissible control inputs. For each $c \in \mathbb{R}_+$ let Ω_c be the sublevel set of V such that

$\Omega_c := \{x \in \mathbb{R}^n : V(x) \leq c\}$. If there exists a $c_i > 0$ such that

$$\inf_{u \in U} L_f V(x) + L_g V(x)u < 0 \quad (3)$$

is satisfied $\forall x \in \Omega_{c_i} \setminus \{0\}$, then the system is locally stabilizable and Ω_{c_i} is a control invariant subset of the Region of Attraction (RoA) of the origin.

Proof. See [18, Proposition 2.2] for the proof of stabilizability. The control invariance proof is straightforward since for any x at the boundary of Ω_c we can always find a $u \in U$ such that $\dot{V}(x, u) < 0$ from condition (3). \square

We can now take c_{max} as the maximum value of $c_i \in \mathbb{R}_+$ such that (3) holds for any $x \in \Omega_{c_i} \setminus \{0\}$. Then, $\Omega_{c_{max}}$ is the largest sublevel set of V contained in the RoA.

Remark 1. We are also allowed to use a recent definition of “local” Control Lyapunov Function [19] instead of the stricter one in Definition 1 and can reach the same conclusion as in Lemma 1. The main benefit of using the local CLF is a higher flexibility in constructing V , since (2) is not required to be satisfied globally.

We can also consider a stronger notion of stabilizability by imposing exponential convergence to the origin. It is well-known that if there exists a compact subset $D \subseteq \Omega_{c_{max}}$ such that $\forall x \in D$ the following holds for some constant $\lambda > 0$,

$$\inf_{u \in U} L_f V(x) + L_g V(x)u + \lambda V(x) \leq 0, \quad (4)$$

then the state of the system can be driven exponentially fast to the origin from any initial state $x_0 \in \Omega_{c_{exp}} \subseteq D$ [20]. If such $c_{exp} > 0$ exists, we will say that V is a *locally exponentially stabilizing* CLF. The condition (4) can be incorporated as a constraint into a min-norm optimization problem:

CLF-QP:

$$u^*(x) = \arg \min_{u \in U} u^T u \quad (5a)$$

$$\text{s.t.} \quad L_f V(x) + L_g V(x)u + \lambda V(x) \leq 0 \quad (5b)$$

which is a quadratic program (QP) if the input constraints are linear. We will refer to constraint (5b) as the *exponential CLF constraint*. This optimization problem defines a feedback control law $u^*: \mathbb{R}^n \rightarrow \mathbb{R}^m$ selecting the smallest possible input such that the system state converges to the origin exponentially quickly. Note that, in practice, constraint (5b) is relaxed in order to guarantee the feasibility of the problem if condition (4) is not locally satisfied [3].

B. Effects of Model Uncertainty on CLF-based Controllers

The main problem concerned in this paper is how to reformulate the min-norm stabilizing controller defined in (5) in the presence of model uncertainty.

First, we provide some necessary settings and assumptions for our problem formulation. Let’s assume that we have a *nominal model*

$$\dot{x} = \tilde{f}(x) + \tilde{g}(x)u, \quad (6)$$

where $\tilde{f} : \mathbb{R}^n \rightarrow \mathbb{R}^n$, $\tilde{g} : \mathbb{R}^n \rightarrow \mathbb{R}^{n \times m}$ are Lipschitz continuous vector fields and $\tilde{f}(0) = 0$. \tilde{f} and \tilde{g} are in general different from the true plant vector fields f and g in (1) but they are related by the following assumption:

Assumption 1. We assume that V in (5), which is verified to be a locally exponentially stabilizing CLF for the nominal model, is also locally exponentially stabilizing for the plant.

Assumption 2. We also assume that we have access to measurements of state and control input at every sampling time Δt .

Our main objective is to construct the exponential CLF constraint (5b) for the true plant when we only know the model dynamics \tilde{f} and \tilde{g} . Since $\dot{V}(x, u) = L_f V(x) + L_g V(x)u$ depends on the dynamics of the plant, the estimate based on the nominal model $\tilde{V}(x, u) = L_{\tilde{f}} V(x) + L_{\tilde{g}} V(x)u$, will differ from its true value. We define $\Delta : \mathbb{R}^n \times \mathbb{R}^m \rightarrow \mathbb{R}$ as the difference between these:

$$\Delta(x, u) := \dot{V}(x, u) - \tilde{V}(x, u). \quad (7)$$

Then, the exponential CLF constraint (5b) becomes

$$L_{\tilde{f}} V(x) + L_{\tilde{g}} V(x)u + \Delta(x, u) + \lambda V(x) \leq 0. \quad (8)$$

Therefore, verifying the exponential CLF constraint for the true plant amounts to a problem of learning the mismatch term $\Delta(x, u)$ correctly and then enforcing (8). We can learn this function from the past data by formulating a supervised learning problem. Specifically, we will use GP regression, a method that will be introduced in the next section which permits to analyze the confidence of the prediction.

Remark 2. In (7), if we express \dot{V} and \tilde{V} with their respective Lie derivatives, we get

$$\Delta(x, u) = \underbrace{(L_f V(x) - L_{\tilde{f}} V(x))}_{=: \Delta_1(x)} + \underbrace{(L_g V(x) - L_{\tilde{g}} V(x))u}_{=: \Delta_2(x)}. \quad (9)$$

Note that we do not have access to $\Delta_1(x)$ and $\Delta_2(x)$ in this equation since we are unaware of f and g . It is tempting to learn each of these terms separately with supervised learning. However, we can only measure $\Delta(x, u)$, which makes this approach intractable. Nevertheless, we can exploit the fact that the mismatch term $\Delta(x, u)$ is control-affine.

III. GAUSSIAN PROCESS REGRESSION

A Gaussian Process (GP) is a random process such that any finite selection of samples $\{h(x_k)\}_{k=1}^n$ has a joint Gaussian distribution. A GP is fully determined by its mean function $m(x)$ and covariance function $k(x, x')$, i.e.,

$$h(x) \sim \mathcal{GP}(m(x), k(x, x')), \quad (10)$$

where $h(x)$ is the output function sampled from the GP. Any positive definite kernel function² can be a valid covariance function [21]. In a function space view, such $k(x, x')$

² $k : \mathcal{X} \times \mathcal{X} \rightarrow \mathbb{R}$ is a positive definite kernel if its associated kernel matrix K is positive semi-definite.

prescribes a specific class of Hilbert space called Reproducing Kernel Hilbert Space (RKHS, [21])³, denoted as $\mathcal{H}_k(\mathcal{X})$, where \mathcal{X} is the domain of the kernel function, a connected subset of \mathbb{R}^n . Moreover, the RKHS norm $\|h\|_k := \sqrt{\langle h, h \rangle_{\mathcal{H}_k}}$, which will be used in Lemma 2, is a measure of its smoothness with respect to the kernel function⁴.

GPs encode prior distributions over functions and given new query points, a posterior distribution can be derived from the joint Gaussian distribution between the prior data and the query points. This gives rise to their typical application in the machine learning literature: GP regression. Given the input-output data pairs $\{(x_j, z_j)\}_{j=1}^N$, the regressor is provided by the posterior GP distribution conditioned on the data. Here, the output data is assumed to be measurements of $h(x_j)$ with additive white noise, i.e., $z_j = h(x_j) + \varepsilon_j$, where $\varepsilon_j \sim \mathcal{N}(0, \sigma_n^2)$. Then, the mean and the variance of the posterior $h(x_*)$ at a query point x_* , are given as

$$\mu_* = \mathbf{z}^T (K + \sigma_n^2 I)^{-1} K_*^T, \quad (11)$$

$$\sigma_*^2 = k(x_*, x_*) - K_* (K + \sigma_n^2 I)^{-1} K_*^T, \quad (12)$$

which are derived from the Joint Gaussian distribution of $\{z_j\}_{j=1}^N$ and $h(x_*)$, where K is the Gram matrix whose (i^{th}, j^{th}) element is defined as $k(x_i, x_j)$, and $K_* = [k(x_*, x_1), \dots, k(x_*, x_N)]$ [22]. $\mathbf{z} \in \mathbb{R}^N$ is the vector containing the output measurements z_j . Note that there exist various choices of kernel functions and many of them depend on some hyperparameters which determine the kernel's characteristics. Depending on the choice of kernel and hyperparameters, the result of the regression varies, and the problem of choosing the best kernel and its hyperparameters is known as the “training” process of the GP regression. In this work, we use marginal likelihood maximization, which is one of the most common training methods [22].

After training, one would like to study how close the GP model approximates the target function. In order to do this, we use the Upper Confidence Bound (UCB) analysis [23], specifically, the following lemma.

Lemma 2. [23, Thm. 6] Assume that the noise sequence $\{\varepsilon_j\}_{j=1}^\infty$ is zero-mean and uniformly bounded by σ_n . Let the target function $h : \mathcal{X} \rightarrow \mathbb{R}$ be a member of $\mathcal{H}_k(\mathcal{X})$ associated with a bounded kernel k , with its RKHS norm bounded by B . Then, with probability of at least $1 - \delta$, the following holds for all $x \in \mathcal{X}$ and $N \geq 1$:

$$|\mu_* - h(x_*)| \leq (2B^2 + 300\gamma_{N+1} \ln^3((N+1)/\delta))^{0.5} \sigma_*,$$

where γ_{N+1} is the maximum information gain after getting $N+1$ data points, and μ_* , σ_*^2 are the mean and variance of the posterior GP given by (11) and (12).

Proof. See [23, Thm. 6]. □

³Intuitively, kernels can be used to define functions on \mathcal{X} , and such space of functions is known as the RKHS. It is called “reproducing” because the inner product between $h \in \mathcal{H}_k$ and $k(\cdot, x)$ reproduces h , i.e., $\langle h(\cdot), k(\cdot, x) \rangle_{\mathcal{H}_k} = h(x), \forall x \in \mathcal{X}$.

⁴ $\|h(x) - h(y)\|_2 \leq \|h\|_k \|k(x, \cdot) - k(y, \cdot)\|_k$

In this lemma, the assumption about the boundedness of $\|h\|_k$ implicitly requires a “low complexity” of the target function [24]. B is usually unknown a priori, but a trial-and-error approach to find its value suffices in practice [23]. γ_{N+1} quantifies the reduction of uncertainty about h in terms of entropy. It has a sublinear dependency on N for many commonly used kernels and it can be efficiently approximated up to a constant [23].

IV. GP REGRESSION FOR AFFINE TARGET FUNCTIONS

In this section, we use GP regression to learn the mismatch term $\Delta(x, u)$ (7) from data. A naive way to do this is to model Δ as some general nonlinear function of x and u , sampled from a GP with some kernel function. However, from (9), we know that it is affine in u . If we use an arbitrary kernel, we cannot exploit this information in our GP regression. Therefore, our first objective must be to construct an appropriate kernel that can incorporate the control-affine structure of Δ in the regression. In order to do this, first, we introduce the general formulation of this problem. Consider m functions, $h_i : \mathcal{X} \rightarrow \mathbb{R}$ for $i = 1, \dots, m$, and define

$$h_c(x, y) := [h_1(x) \ h_2(x) \ \dots \ h_m(x)] \cdot y, \quad (13)$$

where $y \in \mathbb{R}^m$. Our objective is to estimate the function $h_c(x, y) : \mathcal{X} \times \mathbb{R}^m \rightarrow \mathbb{R}$ which is affine in y by using GP regression, given its measurements $z_j = h_c(x_j, y_j) + \varepsilon_j$ for $j = 1, \dots, N$.

The underlying structure of $h_c(x, y)$ tells us that it contains information about m random functions $\{h_i(x)\}_{i=1}^m$ condensed to a single scalar value by a product with y . Therefore, it is natural to consider m underlying kernels and an appropriate composition of them. For $i = 1, \dots, m$, consider covariance functions $k_i : \mathcal{X} \times \mathcal{X} \rightarrow \mathbb{R}$.

Definition 2. *Affine Dot Product Compound Kernel:* Define k_c given by

$$k_c \left(\begin{bmatrix} x \\ y \end{bmatrix}, \begin{bmatrix} x' \\ y' \end{bmatrix} \right) := y^T \text{Diag}([k_1(x, x'), \dots, k_m(x, x')]) y', \quad (14)$$

as the *Affine Dot Product* (ADP) compound kernel of m individual kernels $k_1(x, x'), \dots, k_m(x, x')$.

Note that for a fixed (x, x') , the ADP compound kernel resembles the well-known dot product kernel, defined as $k(y, y') = y^T y'$ [22].

Lemma 3. If k_1, \dots, k_m are positive definite kernels, the ADP compound kernel k_c is also positive definite. Furthermore, if k_1, \dots, k_m are bounded kernels, k_c is also a bounded kernel.

Proof. Consider the Gram matrix of k_c , $K_c \in \mathbb{R}^{N \times N}$ for $\{(x_j, y_j)\}_{j=1}^N$. Let K_i be the Gram matrix of k_i for $\{x_j\}_{j=1}^N$. Define $Y := [y_1 \ y_2 \ \dots \ y_N] \in \mathbb{R}^{m \times N}$, and let \mathbf{y}_i^T be the i -th row of Y . Then,

$$K_c = \sum_{i=1}^m (\mathbf{y}_i \ \mathbf{y}_i^T) \circ K_i,$$

where \circ indicates the Hadamard product [25]. By the Schur Product Theorem [25], if the k_i are positive definite kernels,

then since each $\mathbf{y}_i \mathbf{y}_i^T$ and K_i are positive semidefinite, K_c is a positive semidefinite matrix. Therefore, k_c is a positive definite kernel by definition. Also, if the k_i are bounded kernels, each K_i is bounded so K_c is also bounded. Therefore, k_c is a bounded kernel. \square

By Lemma 3, since k_c is positive definite, it is a valid covariance function and we can construct a corresponding RKHS, namely $\mathcal{H}_{k_c}(\mathcal{X} \times \mathbb{R}^m)$ [21]. This property of k_c will later be used to derive a confidence bound of the estimate of $\Delta(x, u)$ in Section IV.

Theorem 1. If each $h_i(x)$ is a mutually independent GP with zero mean and covariance function $k_i(x, x')$, i.e., $h_i(x) \sim \mathcal{GP}(0, k_i(x, x'))$ for $i = 1, \dots, m$, then $h_c(x, y)$ defined by (13) is also a GP whose mean is zero and the covariance function is the ADP compound kernel k_c .

Proof. Since h_c is a linear combination of GPs, trivially it is also a GP. For any couple of samples $h_c(x, y)$ and $h_c(x', y')$,

$$\begin{aligned} & \mathbb{E}[h_c(x, y) \cdot h_c(x', y')] \\ &= \mathbb{E} \left[\left(\sum_{i=1}^m y_i \cdot h_i(x) \right) \cdot \left(\sum_{j=1}^m y'_j \cdot h_j(x') \right) \right] \\ &= \sum_{i=1}^m y_i y'_i \mathbb{E}[h_i(x) h_i(x')] + \sum_{i \neq j} y_i y'_j \mathbb{E}[h_i(x) h_j(x')] \\ &= \sum_{i=1}^m y_i y'_i k_i(x, x') + 0 = k_c \left(\begin{bmatrix} x \\ y \end{bmatrix}, \begin{bmatrix} x' \\ y' \end{bmatrix} \right). \end{aligned}$$

\square

The zero in the above equation follows from the mutual independence of $h_i(x)$. From Theorem 1, now we can treat our regression problem the same way as any other kind of general GP regression, but with a specific choice of the kernel structure given by (14).

One caveat of this regression is that depending on the distribution of the inputs y_j in the data, this problem can be underdetermined. For instance, when every y_j is a constant vector and $m \geq 2$, there are infinitely many choices of valid $h_i(x)$ that give the same estimation error. Nevertheless, under our GP regression structure, this evidence of underdetermination is implicitly captured by larger values of the variance of the posterior.

In practice, it is preferable to avoid such underdetermination since we want to reduce the uncertainty of the GP posterior. Therefore, we need to carefully collect the training data to make sure we capture rich enough information about our target function. In Section VI we propose a method for this purpose. In the controls and system identification literature, this is related to the property of persistency of excitation [26].

Finally, the main benefit of exploiting the affine structure in the kernel is revealed in the expressions for the posterior distribution’s mean and variance. Let $X \in \mathbb{R}^{n \times N}$, $Y \in \mathbb{R}^{m \times N}$ be matrices whose column vectors are the inputs x_j and y_j of the collected data, respectively, and let $\mathbf{z} \in \mathbb{R}^N$

be the vector containing the output measurements z_j . Then, plugging them and the ADP compound kernel into (11) and (12) gives the following expressions for the mean and variance of the posterior at a query point (x_*, y_*) :

$$\mu_* = \underbrace{\mathbf{z}^T (K_c + \sigma_n^2 I)^{-1} K_{*Y}^T}_{=: b_*^T} y_*, \quad (15)$$

$$\sigma_*^2 = y_*^T \underbrace{\left(\text{Diag} \left(\begin{bmatrix} k_1(x_*, x_*) \\ \vdots \\ k_m(x_*, x_*) \end{bmatrix} \right) - K_{*Y} (K_c + \sigma_n^2 I)^{-1} K_{*Y}^T \right)}_{=: C_*} y_*. \quad (16)$$

Here, $K_c \in \mathbb{R}^{N \times N}$ is the Gram matrix of k_c for the training data inputs (X, Y) , and $K_{*Y} \in \mathbb{R}^{m \times N}$ is given by

$$K_{*Y} = \begin{bmatrix} K_{1*} \\ K_{2*} \\ \vdots \\ K_{m*} \end{bmatrix} \circ Y, \quad K_{i*} = [k_i(x_*, x_1), \dots, k_i(x_*, x_N)].$$

Readers can observe that (15) and (16) are affine and quadratic in y_* , respectively. These structures are critical when formulating the uncertainty-aware CLF chance constraint as a second-order cone constraint in the next section.

V. UNCERTAINTY-AWARE MIN-NORM STABILIZING CONTROL

A. Probabilistic Bounds on the CLF Derivative

We have already presented all the necessary tools to verify the probabilistic bounds on the mismatch term Δ (9). Indeed, learning Δ corresponds to the GP regression problem defined by (15), (16), in which the target function h_c is Δ , x is the state, $y = [1, u^T]^T$, h_1 is Δ_1 , and h_2 is Δ_2 .

Assumption 3. Let \mathcal{H}_{k_1} and \mathcal{H}_{k_2} be RKHSs whose respective associated kernels k_1 and k_2 are bounded. We assume that both Δ_1 and Δ_2 have bounded RKHS norm with respect to \mathcal{H}_{k_1} and \mathcal{H}_{k_2} , respectively.

Lemma 4. Under Assumption 3 and with a compact set of admissible control inputs U , Δ has bounded RKHS norm with respect to \mathcal{H}_{k_c} , namely $\|\Delta\|_{k_c} \leq B$, where k_c is the ADP compound kernel of k_1 and k_2 .

Proof. The proof follows from Definition 2. \square

Assumption 4. We have access to measurements $z_i = \dot{V}(x_i, u_i) - (L_{\bar{f}}V(x_i) + L_{\bar{g}}V(x_i)u_i) + \varepsilon_i$, and the noise term ε_i is zero-mean and uniformly bounded by σ_n . Also, Δ is a member of \mathcal{H}_{k_c} .

With Assumptions 3, 4 and Lemma 4, we can now apply Lemma 2 to our regression problem.

Theorem 2. Let Assumptions 3 and 4 hold. Let $\beta := (2B^2 + 300\gamma_{N+1} \ln^3((N+1)/\delta))^{0.5}$, with N the number of data points, and γ_{N+1} as defined in Lemma 2. Let μ_* and σ_*^2 be the mean and variance of the posterior for Δ using the ADP compound kernel, at a query point (x_*, u_*) as obtained

from (15) and (16). Then, with probability at least $1 - \delta$ the following holds for all $N \geq 1$, $x \in \mathbb{R}^n$, $u \in U$:

$$|\mu_* - \Delta(x_*, u_*)| \leq \beta\sigma_*. \quad (17)$$

Proof. Proof follows from Lemmas 2, 3 and 4. \square

The error in the estimation of the mismatch term Δ is now bounded with some confidence level. From (17) we can easily derive the bounds on the true derivative of the CLF for a probability at least $1 - \delta$:

$$\tilde{V}(x_*, u_*) + \mu_* - \beta\sigma_* \leq \dot{V}(x_*, u_*) \leq \tilde{V}(x_*, u_*) + \mu_* + \beta\sigma_*. \quad (18)$$

B. GP-Based CLF Second-Order Cone Program

Taking the upper bound of (18), we can enforce a chance constraint which guarantees that the CLF will exponentially decay with probability at least $1 - \delta$, and incorporate it into a min-norm optimization problem with linear input constraints $u \in U$. Thus, we can formulate the optimization problem that defines a feedback control law $u^* : \mathbb{R}^n \rightarrow \mathbb{R}^m$ pointwise:

GP-CLF-SOCP:

$$\begin{aligned} u^*(x) = & \arg \min_{u \in U, d} \quad u^T u + p d^2 \\ \text{s.t.} \quad & \tilde{V}(x, u) + \mu_*(x, u) + \beta\sigma_*(x, u) + \lambda V(x) \leq d \end{aligned} \quad (19)$$

Note that this optimization problem does not require knowledge about the true plant dynamics. The stability constraint is relaxed in order to guarantee the feasibility of the problem. With a slight abuse of notation, $\mu_*(x, u)$ and $\sigma_*(x, u)$ are the mean and standard deviation of the GP posterior at (x, u) , obtained from (15) and (16). The fact that μ_* and σ_*^2 are affine and quadratic in u , respectively, is crucial for the following main result of the paper:

Theorem 3. Using the proposed ADP compound kernel, the uncertainty-aware optimization problem (19) is convex, meaning that its global minimum can be reliably recovered. Specifically, it is a Second-Order Cone Program (SOCP).

Proof. Let's first transform the quadratic objective function into a second-order cone constraint and a linear objective. Let the objective function be $J(u, d) := u^T u + p d^2$. Note that by taking $\varphi = [u^T, d]^T$ we can express the objective as $J(\varphi) = \varphi^T Q \varphi$. Next, by setting $z := L\varphi$, where L is the matrix square-root of Q , we can rewrite $J(z) = \|z\|_2^2$. Note that minimizing J gives the same result as minimizing $J'(z) := \|z\|_2$. Now we can move the objective function J' into a second-order cone constraint by setting $\|z\|_2 \leq t$ and minimizing the new linear objective function $J''(t) := t$.

The next step is to prove that the CLF chance constraint is a second-order cone constraint. Note that $\tilde{V}(x, u) = L_{\bar{f}}V(x) + L_{\bar{g}}V(x)u$ and $\mu_*(x, u) = b_*^T [1, u^T]^T$ are both control-affine. Note that $\sigma_*(x, u) = \sqrt{[1, u^T] C_*(x) [1, u^T]^T}$ can be rewritten as $\sigma_*(x, u) = \|M(x)u + n(x)\|_2$, although

we omit the expressions of M and n for conciseness. Therefore, the CLF chance constraint is a second-order cone constraint, and the resulting optimization problem is an SOCP with two second-order cone constraints corresponding to the original objective function and the CLF chance constraint. SOCPs are inherently convex. \square

Remark 3. Note that if the initial state x_0 is outside the CLF maximum sublevel set for exponential stability $\Omega_{c_{exp}}$, we cannot guarantee exponential convergence and neither can the controller which uses the true plant dynamics. However, even for this case, we still do guarantee that the approximation error of the CLF derivative is bounded as given by (18) with probability $1 - \delta$. Also, (19) is always feasible due to the relaxation.

VI. DATA COLLECTION

In this section, we introduce an algorithm that efficiently collects measurements of Δ for the GP regression. This data should contain rich enough information about Δ , especially about its dependency on u as discussed in Section IV, and since our goal is to obtain a locally stabilizing controller, data from outside the RoA should be excluded for efficiency.

To this end, we propose an algorithm that iteratively collects new data and trains a new GP model in an episodic learning fashion. The algorithm uses the level sets of the CLF as “guides” for expanding the training region by exploiting Lemma 1. In addition, we use the idea of greedy search in the Bayesian Optimization literature [23] to actively explore the most uncertain area of the training region. Our algorithm is based on the active learning algorithm of [27], although while [27] focuses on guaranteeing safety online, our objective is to maximize the efficiency of the offline data collection.

A. Discrete-Time Measurements

To start with, first consider how to obtain inputs (x_j, u_j) and labels (z_j) —measurements of $\Delta(x_j, u_j)$ —of the training data. Let $x(t)$ and $u(t)$ be the state and control input measurements at time t and $x(t + \Delta t)$ be the state measurement at the next timestep. We can use these values to create input-label pairs with $\mathcal{O}(\Delta t^2)$ approximation error:

$$\begin{aligned} x_j &= \frac{x(t + \Delta t) + x(t)}{2}, \quad u_j = u(t), \\ z_j &= \frac{V(x(t + \Delta t)) - V(x(t))}{\Delta t} - \tilde{V}(x_j, u_j). \end{aligned}$$

Note that x_j is the average of $x(t)$ and $x(t + \Delta t)$, u_j is the control input during the interval $[t, t + \Delta t]$, and z_j is the difference between the value of $\tilde{V}(x_j, u_j)$ obtained from numerical differentiation and the nominal model-based estimate.

B. Estimation of the Region of Attraction

Next, we introduce a new certificate with the learned uncertainty for a conservative estimation of the RoA. Notice that the condition for inclusion in the RoA provided by Lemma 1, is only valid when there is no model-plant mismatch. Thus, we have to incorporate the learned uncertainty

terms from Section IV as we do when we formulate the GP-CLF-SOCP in Section V.

Theorem 4. Taking the GP posterior distribution from the training data $\{(x_j, u_j, z_j)\}_{j=1}^N$, and β from (17), if there exists a $c > 0$ such that for all $x \in \Omega_c$ it holds that

$$\inf_{u \in U} \tilde{V}(x, u) + \mu_*(x, u) + \beta \sigma_*(x, u) < 0, \quad (20)$$

then Ω_c is in the RoA with probability at least $(1 - \delta)$.

Proof. See [11, Lemma 6]. \square

Notice that this certificate is “conservative” in the sense that it takes the worst-case bound of the effect of the uncertainty term, based on the collected data. Therefore, if we obtain more data and improve our GP model to have less uncertainty, then the conservatism will reduce and we will be able to verify a bigger subset of the RoA. This is the central principle of the algorithm.

C. Algorithm Overview

Finally, we give an overview of the proposed algorithm.

1) *Initial GP Model:* We start considering a level set Ω_{c_0} which is small-enough to be a subset of the RoA (Fig 1.a). Such $c_0 > 0$ always exists due to Assumption 1. We collect an initial batch of training data (D_0) from a set of trajectories whose initial states are randomly sampled from Ω_{c_0} , and train an initial GP regression model. Here, we use the nominal model-based CLF-QP from (5) as our stabilizing controller.

2) *Episodic Learning:* The main loop of our algorithm consists of a series of episodes, and each i -th episode is mainly composed of three steps. 1) In the first step (Fig. 1.b), we obtain a set of N_e points in $(\Omega_{(c_{i-1} + \Delta c_i)} \setminus \Omega_{c_{i-1}}) \times \mathcal{U}$ at which the variance of the posterior of the current GP model is maximal. Δc_i is the parameter that determines the size of the new exploration region. 2) Next (Fig 1.c), we run short rollouts by taking each point from step 1 as our initial state and initial control input. During the rollouts, we also evaluate the stabilizability condition (20) at each timestep. Note that such evaluation is a feasibility problem which is also an SOCP since (20) is a second-order cone constraint. After the rollouts, we expand the level of V (we determine c_i) up to a point for which (20) becomes infeasible. 3) Finally (Fig 1.d), we add the data obtained from the trajectories within Ω_{c_i} to our data set, and train the next GP regression model.

Remark 4. In step 2 of an episode, we check condition (20) only for finite sampled states in $\Omega_{c_i} \setminus \Omega_{c_{i-1}}$, whereas Theorem 4 requires (20) to be satisfied at every state in Ω_{c_i} . Notice that brute-force verification for the whole region of Ω_{c_i} will scale poorly with state dimension. So even though we do not have the rigorous guarantee of Theorem 4, we emphasize that the evaluation points in step 2 are the ones where it is most likely that condition (20) will not be satisfied, since they have the highest values of σ_* . Therefore, in practice, we observe that this algorithm can well approximate c_{max} such that $\Omega_{c_{max}}$ is contained in the true RoA (See Fig. 1(e)).

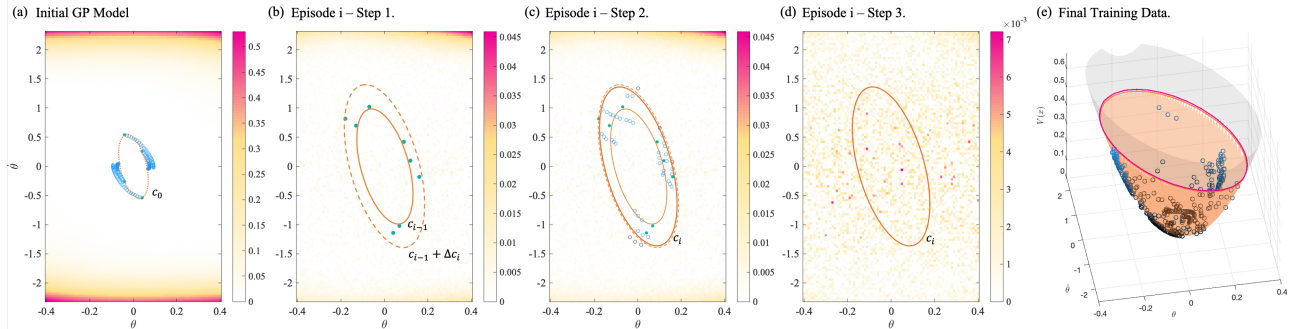


Fig. 1. Visualization of the episodic learning data collection algorithm running on the inverted pendulum example: Color map represents the maximum variance of posterior GP, $\max_{u \in U} \Delta_*(x, u)$. Orange curves: level curves of the CLF. Green points: initial states for the rollouts, Blue points: trajectory points added to the training data. Grey points: trajectory points excluded from the training data. (a) **Initial GP Model:** Trajectories sampled from the initial level set Ω_{c_0} by running CLF-QP are collected to create an initial GP model. (b) **Episode i-Step 1:** N_e initial states and initial control inputs in $(\Omega_{(c_{i-1} + \Delta c_i)} \setminus \Omega_{c_{i-1}}) \times \mathcal{U}$ are determined where σ_* are maximal. (c) **Episode i-Step 2:** Simulations are run from such initial points and the resulting trajectories are saved. At the same time, c_i is determined by evaluating (20) for the sampled trajectories. (d) **Episode i-Step 3:** Finally, the i -th GP model is updated. Note the reduction in the variance. (Total episodes = 7, $i = 3$ for (b), (c), (d).) (e) **Distribution of the final training data** plotted in $x-V(x)$ space (blue points). Level curve in color magenta is the $\Omega_{c_{max}}$ (maximum level set contained in the ROA) for the true plant. The value of CLF is plotted in grey and the orange region is the region verified as RoA through the data collection algorithm.

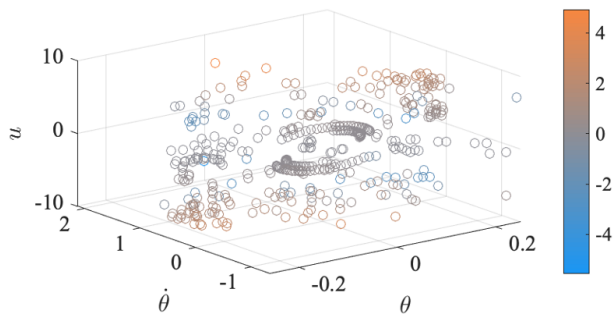


Fig. 2. Distribution of the training data for inverted pendulum example, plotted in $x-u$ space. Color indicates the value of z_i , the measurement of $\Delta(x_i, u_i)$. The number of data points is 425.

VII. EXAMPLES

Having presented the uncertainty-aware min-norm stabilizing controller GP-CLF-SOCP, together with an efficient data-collection algorithm, we proceed to validate the proposed methods using numerical simulations.

A. Two-dimensional System: Inverted Pendulum

Consider a control-affine two-dimensional inverted pendulum as the one in [27], with parameters of the plant $m_{\text{plant}} = 2\text{kg}$, $l = 1\text{m}$ and for the model, $m_{\text{model}} = 1\text{kg}$, $l = 1\text{m}$, which results in model uncertainty in both f and g in (1).

A CLF-QP controller (5) based on the nominal model is designed to stabilize the pendulum to the upright position. In order to illustrate the effects of model uncertainty, we compare it with the CLF-QP controller based on the true plant dynamics. The difference between the two controllers (Fig. 3) is due to the effects of model uncertainty. Specifically, in this case the model uncertainty makes the system converge more slowly.

Fig. 1 and Fig. 2 depict the data collection algorithm and the resulting training data, respectively, for the GP model for GP-CLF-SOCP. The results of deploying the GP-CLF-SOCP controller, with a confidence level of $1-\delta=0.95$, are presented in Fig. 3 in blue lines. Note that the results are very

similar to those from the CLF-QP based on the true plant dynamics, which means that the GP-CLF-SOCP successfully captures the correct effects of model uncertainty. Also, the computation time of the GP-CLF-SOCP, including the GP inference time, is $9.1 \pm 2.2\text{ms}$ (max: 25.7ms) on a laptop with a 10th-gen Intel Core i7 and 32GB RAM.

In order to benchmark the GP-CLF-SOCP, we compare its performance with the one obtained if we only learn the uncertainty in f , as done in previous works [13], [15]. For this, we design a GP-based Control Lyapunov Function Quadratic Program (GP-CLF-QP) that only learns the uncertainty Δ_1 in (9). The results of this controller are also shown in Fig. 3. Additionally, we have compared both controllers when there is actually no uncertainty in $g(x)$, in which case the GP-CLF-SOCP and GP-CLF-QP generate almost identical trajectories, very close to those of the true plant-based CLF-QP.

B. System with Multiple Control Inputs: Kinematic Bicycle

Next, in order to show that our method can be successfully applied to systems with higher state dimension and multiple control inputs, we apply it to track a reference trajectory using a kinematic bicycle model. The state is defined as $x = [p_x, p_y, v, \theta, \gamma]^T$ (p_x, p_y : position coordinates, v : speed, θ : heading angle, γ : tangent of the steering angle). The dynamics of the system are given as

$$\dot{x} = f(x) + g(x)u, \quad f(x) = \begin{bmatrix} v \cos \theta \\ v \sin \theta \\ -f_\mu \\ v \gamma \\ 0 \end{bmatrix}, \quad g(x) = \begin{bmatrix} 0 & 0 \\ 0 & 0 \\ b_v & 0 \\ 0 & 0 \\ 0 & b_\gamma \end{bmatrix}, \quad (21)$$

where $u \in \mathbb{R}^2$, and f_μ , b_v , b_γ are constants that emulate friction and skid effects. For the nominal model, we assume no such effects ($f_\mu = 0$, $b_v = b_\gamma = 1$) and for the plant, we use $f_\mu = 1$, $b_v = 1.5$, $b_\gamma = 0.75$. The objective is to stabilize to a constant-velocity trajectory along the x-axis; $v(t) = 5$, $p_y(t) = \theta(t) = \gamma(t) = 0$. The initial state is set as $x_0 = [0, 0.25, 2, 0.25, 0.25]^T$.

Fig. 4 shows the simulation results of the GP-CLF-SOCP and those of the CLF-QP based on the nominal model and

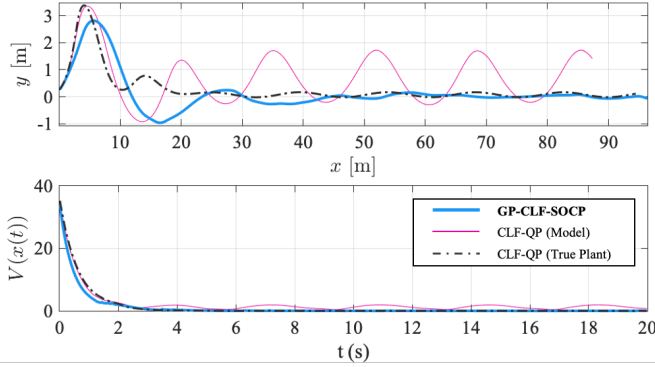


Fig. 4. Trajectories in x – y plane (Top) and histories of $V(x(t))$ (Bottom) of the kinematic vehicle under artificial drift and friction. Comparison between GP-CLF-SOCP, CLF-QP(Model), and CLF-QP(Plant). The sampling time is set as 20ms, and the computation time of the GP-CLF-SOCP per timestep is 10.3 ± 1.9 ms (max: 20.4ms). Number of training data points for GP-CLF-SOCP: 961.

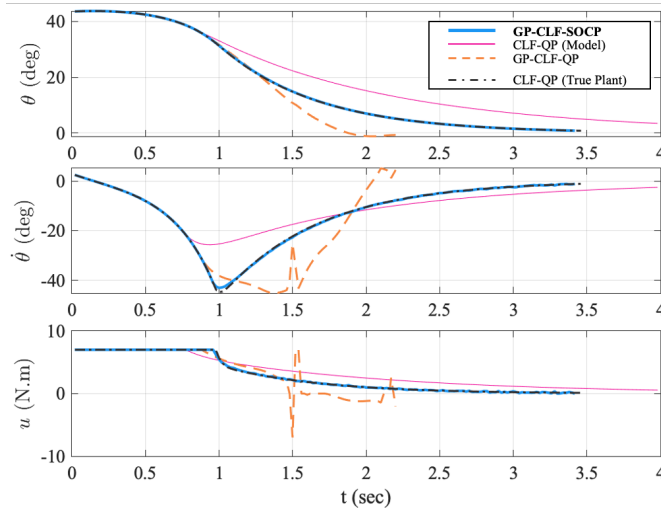


Fig. 3. Simulation of GP-CLF-SOCP for inverted pendulum with model-plant mismatch of $m_{\text{plant}} = 2\text{kg}$, $m_{\text{model}} = 1\text{kg}$, compared to nominal-model-based CLF-QP, and GP-CLF-QP that models uncertainty to be unaffected by u . Results of CLF-QP based on the true plant are also provided to show that GP-CLF-SOCP learns the correct exponential CLF constraint.

the true plant. Here, we use a polynomial CLF [28], which is verified to be locally stabilizing for the nominal model. While the nominal model-based CLF-QP oscillates around the reference trajectory, the GP-CLF-SOCP successfully converges to the reference trajectory.

VIII. CONCLUSION

We have presented a method to design a stabilizing controller for control-affine systems with both state and input-dependent model uncertainty using GP regression. For this purpose, we have proposed the novel ADP compound kernel, which captures the control-affine nature of the problem. This permits the formulation of the so-called GP-CLF-SOCP, which is solved online to obtain an exponentially stabilizing controller with probabilistic guarantees. After testing it on the numerical simulation of two different systems, we obtain a clear improvement with respect to the nominal model-based

CLF-QP and we are able to closely match the performance of the true plant-based controller.

Future work includes exploring the use of sparse GPs to improve the computation time and make the approach more suitable for higher dimensional systems. Also, we can apply our approach to tackle the safety-critical control problem similarly by using Control Barrier Functions [17].

REFERENCES

- [1] Z. Artstein, “Stabilization with relaxed controls,” *Nonlinear Analysis: Theory, Methods and Applications*, vol. 7, pp. 1163 – 1173, 1983.
- [2] E. D. Sontag, “A ‘universal’ construction of artstein’s theorem on nonlinear stabilization,” *Systems and Control Letters*, vol. 13, no. 2, pp. 117 – 123, 1989.
- [3] K. Galloway, K. Sreenath, A. D. Ames, and J. W. Grizzle, “Torque saturation in bipedal robotic walking through control lyapunov function-based quadratic programs,” *IEEE Access*, vol. 3, pp. 323–332, 2015.
- [4] Q. Nguyen and K. Sreenath, “Optimal robust control for bipedal robots through control lyapunov function based quadratic programs,” in *Robotics: Science and Systems*, Rome, Italy, 2015.
- [5] J. Reher, C. Kann, and A. D. Ames, “An inverse dynamics approach to control lyapunov functions,” in *American Control Conference*, 2020.
- [6] A. D. Ames and M. Powell, “Towards the unification of locomotion and manipulation through control lyapunov functions and quadratic programs,” in *Control of Cyber-Physical Systems*. Springer, 2013, pp. 219–240.
- [7] Q. Nguyen and K. Sreenath, “L1 adaptive control for bipedal robots with control lyapunov function based quadratic programs,” in *American Control Conference*, Chicago, IL, July 2015, pp. 862–867.
- [8] A. J. Taylor, V. D. Dorobantu, H. M. Le, Y. Yue, and A. D. Ames, “Episodic learning with control lyapunov functions for uncertain robotic systems,” in *IEEE/RSJ International Conference on Intelligent Robots and Systems*, 2019, pp. 6878–6884.
- [9] J. Choi, F. Castaño, C. Tomlin, and K. Sreenath, “Reinforcement Learning for Safety-Critical Control under Model Uncertainty, using Control Lyapunov Functions and Control Barrier Functions,” in *Robotics: Science and Systems*, Corvallis, OR, July 2020.
- [10] T. Westenbroek, F. Castaño, A. Agrawal, S. S. Sastry, and K. Sreenath, “Learning min-norm stabilizing control laws for systems with unknown dynamics,” *arXiv preprint arXiv:2004.10331*, 2020.
- [11] F. Berkenkamp, R. Moriconi, A. P. Schoellig, and A. Krause, “Safe learning of regions of attraction for uncertain, nonlinear systems with gaussian processes,” in *IEEE Conference on Decision and Control*, 2016, pp. 4661–4666.
- [12] J. Umlauft, L. Pöhler, and S. Hirche, “An uncertainty-based control lyapunov approach for control-affine systems modeled by gaussian process,” *IEEE Control Systems Letters*, vol. 2, pp. 483–488, 2018.
- [13] D. D. Fan, J. Nguyen, R. Thakker, N. Alatur, A.-a. Agha-mohammadi, and E. A. Theodorou, “Bayesian learning-based adaptive control for safety critical systems,” *arXiv preprint arXiv:1910.02325*, 2019.
- [14] R. Cheng, M. J. Khojasteh, A. D. Ames, and J. W. Burdick, “Safe multi-agent interaction through robust control barrier functions with learned uncertainties,” *arXiv preprint arXiv:2004.05273*, 2020.
- [15] L. Zheng, J. Pan, R. Yang, H. Cheng, and H. Hu, “Learning-based safety-stability-driven control for safety-critical systems under model uncertainties,” *arXiv preprint arXiv:2008.03421*, 2020.
- [16] M. J. Khojasteh, V. Dhiman, M. Franceschetti, and N. Atanasov, “Probabilistic safety constraints for learned high relative degree system dynamics,” in *Learning for Dynamics and Control*, 2020, pp. 781–792.
- [17] A. D. Ames, X. Xu, J. W. Grizzle, and P. Tabuada, “Control barrier function based quadratic programs for safety critical systems,” *IEEE Transactions on Automatic Control*, vol. 62, pp. 3861–3876, 2017.
- [18] Y. Lin and E. D. Sontag, “Control-lyapunov universal formulas for restricted inputs,” *Control-Theory and Advanced Technology*, vol. 10, pp. 1981–2004, 1995.
- [19] F. Camilli, L. Grüne, and F. Wirth, “Control lyapunov functions and zubov’s method,” *SIAM Journal on Control and Optimization*, vol. 47, no. 1, pp. 301–326, 2008.
- [20] A. D. Ames, K. Galloway, K. Sreenath, and J. W. Grizzle, “Rapidly exponentially stabilizing control lyapunov functions and hybrid zero dynamics,” *IEEE Transactions on Automatic Control*, vol. 59, no. 4, pp. 876–891, 2014.

- [21] H. Wendland, *Scattered data approximation*. Cambridge university press, 2004, vol. 17.
- [22] C. K. Williams and C. E. Rasmussen, *Gaussian processes for machine learning*. MIT press, Cambridge, MA, 2006, vol. 2, no. 3.
- [23] N. Srinivas, A. Krause, S. Kakade, and M. Seeger, “Gaussian process optimization in the bandit setting: No regret and experimental design,” in *Proceedings of the 27th International Conference on Machine Learning*. Madison, WI, USA: Omnipress, 2010, p. 1015–1022.
- [24] S. R. Chowdhury and A. Gopalan, “On kernelized multi-armed bandits,” in *Proceedings of the 34th International Conference on Machine Learning - Volume 70*, 2017, p. 844–853.
- [25] R. A. Horn, “The hadamard product,” in *Proceedings of Symposia in Applied Mathematics*, vol. 40, 1990, pp. 87–169.
- [26] M. Verhaegen and V. Verdult, *Filtering and system identification: a least squares approach*. Cambridge university press, 2007.
- [27] F. Berkenkamp, M. Turchetta, A. Schoellig, and A. Krause, “Safe model-based reinforcement learning with stability guarantees,” in *Advances in Neural Information Processing Systems*. Curran Associates, Inc., 2017, vol. 30, pp. 908–918.
- [28] H. Ravanbakhsh and S. Sankaranarayanan, “Learning control lyapunov functions from counterexamples and demonstrations,” *Autonomous Robots*, vol. 43, no. 2, p. 275–307, Feb. 2019.